*Int. J. Electrochem. Sci.*, 12 **(2017)** 5742 – 5755, doi: 10.20964/2017.06.27

International Journal of
ELECTROCHEMICAL
SCIENCE
www.electrochemsci.org

# Corrosion Mechanism of Steels in MDEA Solution and Material Selection of the Desulfurizing Equipment

*Tan Sizhou*[1], *Xiao Guoqing*[1,2], *Ambrish Singh*[3,4,*], *Shang Jianfeng*[5], *Long Decai*[1], *Zhang Naiyan*[3], *Zeng Dezhi*[3], *Eno E. Ebenso*[6]

[1]College of Chemical Engineering, Southwest Petroleum University, Chengdu-610500, China
[2]Key Laboratory of Oil and Gas Fire Protection of Sichuan Province
[3]State Key Laboratory of Oil and Gas Reservoir Geology and Exploitation, Southwest Petroleum University, Chengdu, 610500 China
[4]School of Materials Science and Engineering, Southwest Petroleum University, Chengdu-610500, China.
[5]Zhongyuan Oilfield Company, Sinopec, Puyang, 457001, China
[6]Department of Chemistry, School of Mathematical & Physical Sciences, North-West University(Mafikeng Campus), Private Bag X2046, Mmabatho 2735, South Africa.
[*]E-mail: vishisingh4uall@gmail.com; drambrishsingh@gmail.com

*Received:* 9 May 2016 / *Accepted:* 30 March 2017 / *Published:* 12 May 2017

In the present study, the corrosion properties of three steel were evaluated in 45 wt.% Methyldiethanolamine (MDEA) solution, saturated to the hydrogen sulfide ($H_2S$) and carbon dioxide ($CO_2$) as in the oilfields. Corrosion tests were performed using dynamic high temperature (HT) autoclave for various temperature conditions. Corrosion behavior of steels was monitored using electrochemical methods (Tafel polarization and Electrochemical Impedance Spectroscopy). Indoor autoclave loss tests showed that at a lower temperature (40°C ~ 60°C), corrosion rate of 20#, 304L and 316L are low, but increased significantly as the temperature rises. Electrochemical studies suggested that in the MDEA desulfuration solution containing $H_2S$ / $CO_2$, 20 #, 304L and 316L steels are mainly susceptible to $H_2S$ corrosion. With the increase in temperature, the corrosion potentials of the three steels shift negatively, the charge transfer resistance decreases, which accelerate the metal anode dissolution rate significantly.

**Keywords:** MDEA; Steel; EIS; Polarization; XRD; SEM

## 1. INTRODUCTION

Chemical absorption of acid gases, such as $CO_2$, $H_2S$ or $SO_2$ has been widely used in the industrial process. At present, one of the effective methods for the uptake of $CO_2$ usually employs aqueous solutions of alkanolamine or their mixtures, including monoethanolamine (MEA),

diethanolamine (DEA), and N-methyldiethanolamine (MDEA) [1]. Corrosion in alkanolamine gas treating plants begins with the acid gases which are the target of the treating, and is enhanced by several physical and chemical factors. Depending on which the following four amine units were designed to remove the acid gases [2]. The typical amine concentrations, expressed as weight percent of pure amine in the aqueous solution are:

- Monoethanolamine: About 20% for removing $H_2S$ and $CO_2$, and about 32% for removing only $CO_2$.
- Diethanolamine: About 20 to 25% for removing $H_2S$ and $CO_2$
- Methyldiethanolamine: About 30 to 55% for removing $H_2S$ and $CO_2$
- Diglycolamine: About 50 % for removing $H_2S$ and $CO_2$

Refinery amine units utilize aqueous solutions of alkanolamines, such as N-methyldiethanolamine (MDEA), diethanolamine (DEA), and di-isopropanolamine (DIPA), to remove hydrogen sulfide ($H_2S$), carbon dioxide ($CO_2$), carbonyl sulfide (COS) and mercaptans from various product and gas streams. Sulfur recovery unit tail gas clean-up units also use amines, such as MDEA. MDEA solutions have the lowest heat requirements for regeneration because they can be used at 50% strength. Actually, monoethanolamine (MEA) or methyldiethanolamine (MDEA) absorbing $CO_2$ is a typical chemical reaction accompanied with a gas–liquid mass transfer process. Generally, the reaction is kinetics controlled under low concentrations of MEA/MDEA, while it is diffusion controlled under high concentrations of MEA/MDEA [3]. Methyldiethanolamine (MDEA) is a tertiary alkanolamine widely used as absorbent in natural gas sweetening process for removal of hydrogen sulfide ($H_2S$) and carbon dioxide ($CO_2$) [4]. However, $CO_2$ reacts with water to produce carbonic acid which finally reacts with MDEA. Since the reaction of MDEA with $CO_2$ is slow, it hinders the absorption process. Thus, allowing $H_2S$ to be readily absorbed by MDEA solution and making it selective for $H_2S$ removal [5]. Both $H_2S$ and $CO_2$ are acid gases and hence corrosive to carbon steel. However, the Puguang gas field in China, the largest reserves among the discovered gas fields, contains 15% $H_2S$ and 10% $CO_2$. Such huge quantities of acid gases, which bring great challenges to the pipe protection and cause unwished environment problems, should be removed before natural gas downstream processing or distribution.

The objective of the present study was to investigate the three steels under hydrogen sulfide ($H_2S$) and carbon dioxide ($CO_2$) conditions as in the oilfields using autoclave and electrochemical tests to determine the material selection for desulfurizing equipment [6-8]. Also, to study the effect of temperature on corrosion of the three selected steels. Surface study was performed to support the experimental results.

## 2. METHODOLOGY AND EXPERIMENTAL

### *2.1. Materials and specimen preparation*

According to the ASTM standards, the three steel coupons (20, 304L and 316L) were prepared with dimension of 10 mm × 10mm × 5 mm and 30 mm × 15 mm × 3 mm. These samples were used for

electrochemical test and dynamic high temperature (HT) autoclave experiments respectively. The chemical composition of the samples is listed in Table 1.

**Table 1.** Chemical composition of three steel (wt %)

| Element | Cr | Ni | Mo | Mn | Si | S | C | P |
|---|---|---|---|---|---|---|---|---|
| **20#** | 0.00 | 0.00 | 0.00 | 0.51 | 0.22 | 0.028 | 0.220 | 0.012 |
| **304L** | 19.00 | 9.40 | 0.00 | 1.42 | 0.54 | 0.012 | 0.022 | 0.024 |
| **316L** | 17.04 | 11.14 | 2.16 | 1.44 | 0.54 | 0.012 | 0.020 | 0.020 |

*2.2 Electrochemical test*

The electrochemical experiments were evaluated using classic three-electrode system in a PARSTAT2273 electrochemical workstation produced by Princeton Applied Research Company at a constant temperature bath. The cell assembly with electrodes was sealed with epoxy with 1 $cm^2$ contact area that was used as the working electrode; Pt electrode was the counter electrode (CE); the saturated calomel electrode was the reference electrode (RE). All the electrochemical tests were done at different temperatures to get more information on the corrosion rates.

Before the experiment, the working electrode was abraded with SiC paper (240, 360, 800) and then polished with diamond paste through 0.05 um grit, rinsed with distilled water and mineral ether as well as anhydrous ethanol to keep it clean, finally dried.

Polarization curves were obtained by potentiodynamic polarization technology, at a scan rate of 0.5 mV/s. The frequency of electrochemical impedance spectroscopy (EIS) was in the range of 0.1 Hz–100 kHz.

*2.3 Dynamic HT autoclave experiment*

The three samples of 20#, 304L and 316L steel were polished to a mirror finish in order to eliminate scratches, and then cleaned by mineral ether and anhydrous ethanol, finally dried and weighed. The coupons were placed in the high temperature (HT) autoclave, and the oxygen free desulfurization solution (45% MEDA, the rest is water) was poured into it. Simultaneously, autoclave was quickly sealed and pure $N_2$ was used to test pressure. While heating to the experimental temperature, 0.5MPa standard $H_2S$ and $CO_2$ gases (the mass ratio: 1.75) were delivered into the HT autoclave and the flow rate is then set to 1 m/s to start the experiment.

After performing the weight-loss tests, the corrosion products of the specimens were subjected to a detailed analysis by scanning electron microscopy (SEM) and energy dispersive X-Ray spectroscopy (EDX).

## 3. RESULTS AND DISCUSSION

### *3.1 Effect of temperature on electrochemical process*

Polarization curves of three steels measured at different temperatures in the desulfurization solution sutured with $H_2S/CO_2$ are shown in figure 1, and the corresponding fitting results of polarization curve parameters on three steels are listed in table 2.

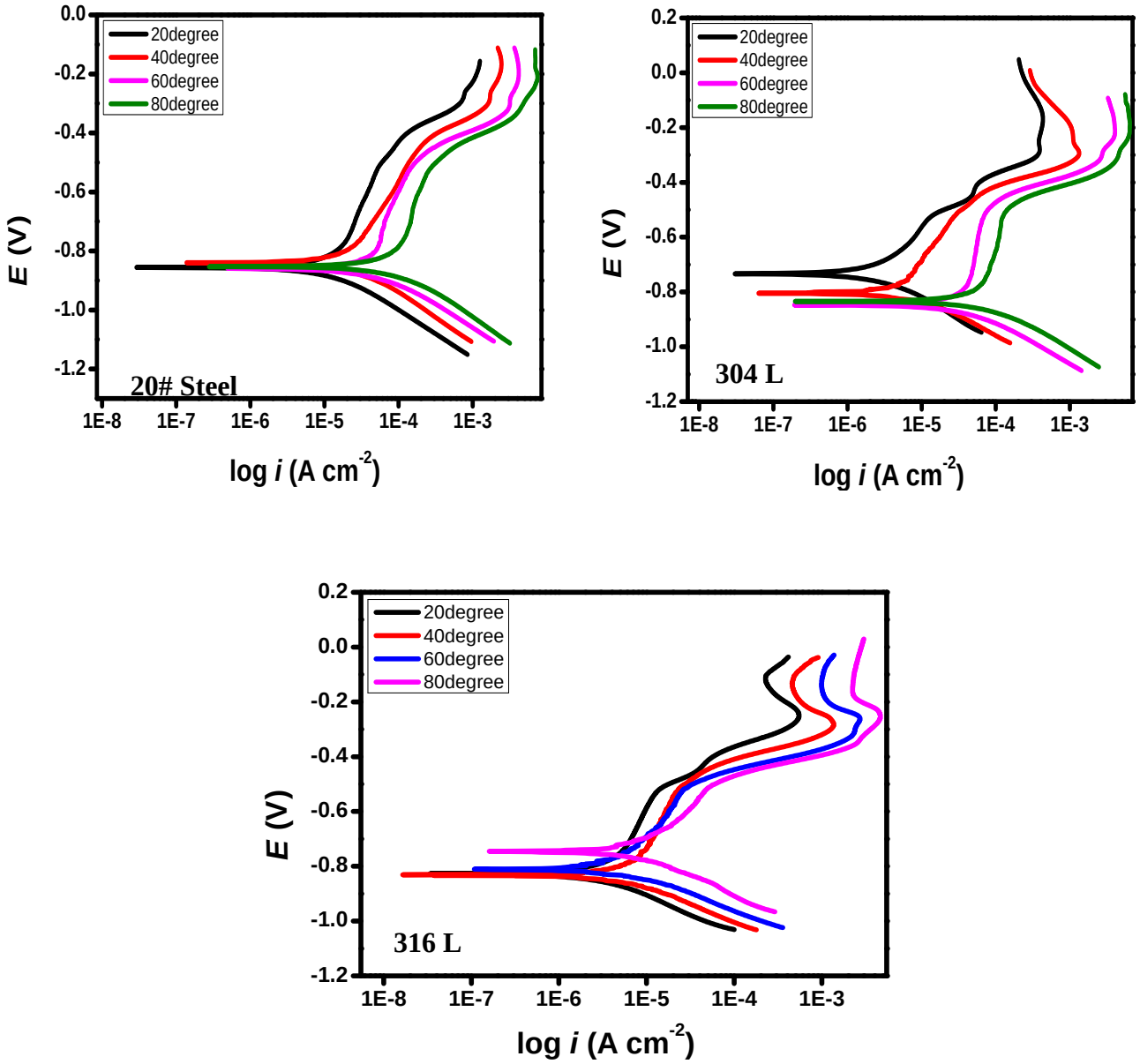


**Figure 1.** Polarization curves at 0.5 mV/s of three steel in the desulfurization solution saturated with $H_2S/CO_2$

Corrosion potential has a great effect on its corrosion tendency, while the corrosion current density is directly related to the corrosion rate of steels. There is an obvious relationship among the

corrosion potential and corrosion current density with the temperature [9-15]. Moreover, the corrosion current density of 20# steel was 0.003879 mA/cm$^2$ at 20° C. However, that of 80° C has increased by nearly 18 times (figure 1 and table 2 (a)). The results indicate that the corrosion process was mainly controlled by the anode (figure 1), and the temperature affected greatly the corrosion speed of 20# steel in MDEA desulfurization solution saturated with $H_2S/CO_2$. It was found that the change in stainless steel is similar to that of 20# steel as well. However, unlike 20# steel, the anode polarization curves (figure 1 (b)) show that passivation phenomenon occurred on 304L steel in desulfurization solution containing acidic components [16-18].

**Table 2.** Electrochemical polarization parameters at 0.5 mV/s for the corrosion of steels in 45% MDEA solution at different temperatures

| Material | Temperature (℃) | $E$ (V) | $b_a$ (mV/dec) | $-b_c$ (mV/dec) | $i_{corr}$ (mA/cm$^2$) |
|---|---|---|---|---|---|
| **20#** | 20 | -0.64487 | 235.74 | 158.72 | 0.003879 |
| | 40 | -0.68933 | 220.25 | 126.91 | 0.004470 |
| | 60 | -0.70217 | 171.49 | 136.66 | 0.022350 |
| | 80 | -0.67238 | 154.73 | 203.54 | 0.068807 |
| | | | | | |
| **304L** | 20 | -0.52159 | 64.203 | 82.06 | 0.000459 |
| | 40 | -0.60775 | 273.70 | 127.04 | 0.002712 |
| | 60 | -0.70342 | 294.19 | 140.02 | 0.003133 |
| | 80 | -0.66942 | 544.31 | 118.05 | 0.009958 |
| | | | | | |
| **316L** | 20 | -0.52064 | 85.11 | 56.689 | 0.000494 |
| | 40 | -0.60848 | 140.42 | 71.618 | 0.001443 |
| | 60 | -0.65829 | 164.59 | 75.987 | 0.003012 |
| | 80 | -0.63427 | 171.71 | 107.82 | 0.009350 |

The dissolution and regeneration is a complex dynamic process, where temperature contributes greatly to the dissolution and regeneration of passive film [19-28]. By comparing figure 1b and c, a similar passivation phenomenon occurred, but the corrosion current density value of 316L is smaller than 304L. All these results showed that the corrosion in 316L steel was steadier than the 304L steel in the present experiment condition.

The corrosion mechanism at the interface between the carbon steel surface and the desulfurization solution sutured with $H_2S/CO_2$ varies from corrosive environments. It mainly includes two corrosive environments ($H_2S$-$CO_2$-$H_2O$ corrosion and $RNH_2$-$H_2S$-$CO_2$-$H_2O$ corrosion). The $H_2S$-$CO_2$-$H_2O$ corrosion in overhead condensing system of regeneration tower in the desulfurizing unit was

deteriorating. Once the acid gases enter the desulfurizing device, it forms wet $H_2S$ environment, which leads to sulphide stress fracture of metal. The process can be summarized as first, $H_2S$ aqueous solution dissociates into $H^+$, $HS^-$ and $S^{2-}$. $H_2S=H^++HS^-$

$HS^-=H^++S^{2-}$

$CO_2+H_2O=H_2CO_3$

$H_2CO_3= HCO_3^-+H^+$

$HCO_3^-= CO_3^{2-}+H^+$

$Fe\rightarrow Fe^{2+}+2e$

$2H^++2e=H_2\uparrow$

$Fe^{2+}+S^{2-}=FeS\downarrow$

$2Fe^{2+}+2HS^-=2FeS\downarrow+ H_2\uparrow$

$Fe^{2+}+CO_3^{2-}=FeCO_3\downarrow$

$Fe^{2+}+2HCO_3^-\rightarrow Fe(HCO_3)_2\rightarrow FeCO_3\downarrow+ H_2O+ CO_2\uparrow$

The $RNH_2$-$H_2S$-$CO_2$-$H_2O$ corrosion is a process, which consists of several operation units for instance, contactor tower, regenerator tower and heat exchanger. The chemical reaction of amines with $H_2S$ and $CO_2$ are given below [29]:

$2RNH_2 + H_2S \rightarrow (RNH_3)_2S$

$(RNH_3)_2S+H_2S \rightarrow 2(RNHS_3)HS$

$2RNH_2+CO_2+H_2O \rightarrow (RNH_3)_2CO_3$

$(RNH_3)_2CO_3+CO_2+H_2O \rightarrow 2(RNH_3)\ HCO_3$

During the transfer process, the corrosion rate of 20# steel was enhanced with the increase in the temperature to speed up its kinetics and thermodynamics of electrode reaction at temperatures below 60°C; this was mainly because increase in temperature accelerated the adsorption, active dissolution on the surface of the metal anode, and speed up hydrogen corrosion. However, when the temperature was above 60°C, the acidic components solubility in the desulfuration solution is reduced especially, when the temperature is 80°C. It can be clearly seen that the air bubbles come out through the desulfurization solution, which results in the concentration decrease of corrosion media such as $H_2S$ and $CO_2$, and adsorption decline of $HS^-$ on the surface of the metal anode. Nevertheless, increase in temperature speeds up significantly the metal dissolution of 20 # steel, the interaction of two factors eventually contributed to increasing corrosion current density and positive steady potential [30].

EIS, as an approach of characterizing a corroding metal in an aqueous medium, is widely used in the corrosion system measurement. Then, impedance spectra were measured at 20°C, 40°C, 60°C and 80°C. The results are illustrated in Figure 2.

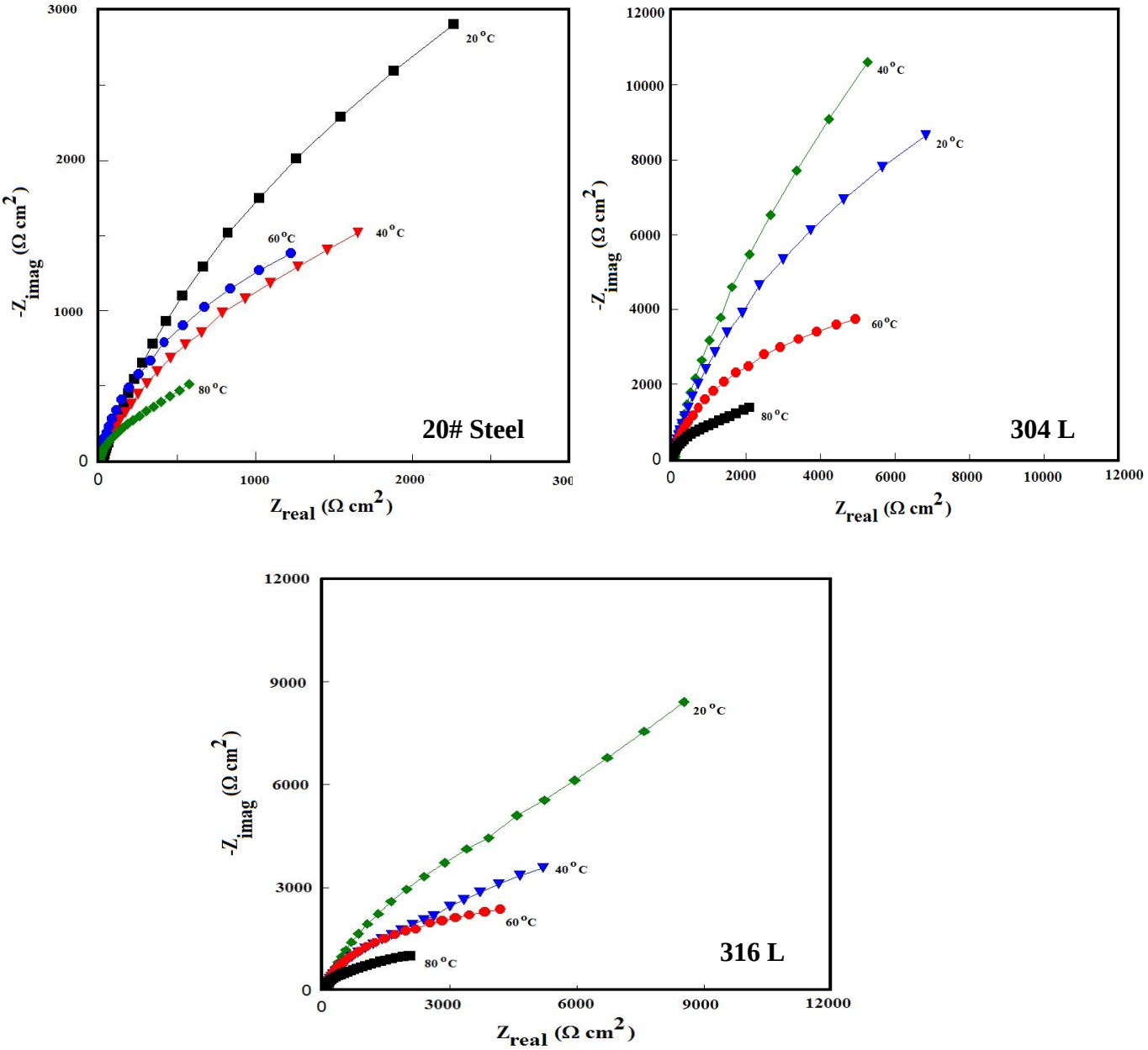


**Figure 2.** Impedance spectra at an amplitude of 10 mV of three steel in MDEA desulfurization solution sutured with $H_2S/CO_2$

From figure 2, the diameter of the measured Nyquist plots of three steels changed with the temperature. The diameter decreased with the increase of the temperature, which can be explained by the decrease of the total charge transfer resistance in electrochemical course.

Table 3 showed that the charge transfer resistance ($R_{ct}$) of 20# steel in desulfurization solution at 20°C was 3349 Ωcm$^2$, while its value decreases to 344.6 Ωcm$^2$ at 80°C. By comparing with stainless steel, the charge transfer resistance of 304L steel in desulfurization solution increased by almost one order of magnitude at 20°C [31].

**Table 3.** Electrochemical impedance spectrum parameters at an amplitude of 10 mV for the corrosion of three steel in 45% MDEA acidic solution at different temperatures

| Material | Temperature (℃) | $R_s$ ($\Omega$•cm$^2$) | $Q$ ($10^{-6}\Omega^{-1}$•S$^n$•cm$^{-2}$) | $n$ | $R_{ct}$ ($\Omega$•cm$^2$) |
|---|---|---|---|---|---|
| **20#** | 20 | 15.83 | 717.2 | 0.7686 | 3349 |
| | 40 | 2.064 | 639.4 | 0.7701 | 1741 |
| | 60 | 4.067 | 490.6 | 0.8141 | 757.6 |
| | 80 | 4.463 | 1392.0 | 0.7448 | 344.6 |
| | | | | | |
| **304L** | 20 | 13.87 | 233.5 | 0.8473 | 23630 |
| | 40 | 1.873 | 296.2 | 0.8791 | 6363 |
| | 60 | 2.263 | 303.1 | 0.8392 | 2978 |
| | 80 | 4.74 | 652.9 | 0.7608 | 892.9 |
| | | | | | |
| **316L** | 20 | 7.62 | 206.0 | 0.8000 | 33740 |
| | 40 | 2.96 | 252.1 | 0.8874 | 9281 |
| | 60 | 2.70 | 284.8 | 0.8351 | 3047 |
| | 80 | 1.50 | 397.9 | 0.6595 | 1289 |

The results show clearly that increase in temperature can largely promote the passivation membrane dissolution of 304L steel. However, the dissolution and formation of passivation film itself is a dynamic process, in which pitting occurred in desulfurizing MDEA solution containing relatively high concentrations of chloride ions. However, compared with 304L steel, there is no significant change in 316L steel. It also indicates that increase in temperature largely promotes the corrosion process and it mainly express in both aspects of accelerating the dissolution of passivation film and solution resistance. The results are in good agreement with the work done by other authors [32-35].

*3.2 Analysis of weight –loss test*

The comparative analysis results of corrosion rate on three different steels (20#, 304L and316L) are demonstrated in figure 3. As is shown in figure 3 there is no significant difference among the corrosion rates of three steel in the desulfurizing MDEA solution at low temperatures (40°C-60°C). In addition, the corrosion rate of 20# steel increased with the rise in temperature (＞ 60°C), then exceeds 0.25 mm/a at 100°C. According to NACE RP0775-05 standard, it is in the range of severe corrosion, while that of another two stainless steels (304L and 316L steel) are slight [36].

It seems from figure 4 that increasing the temperature leads to increase in the corrosion rate. Moreover, for 20# steel, the corrosion rate has an exponential relationship with the temperature, while that of another two stainless steels (304L and 316L) has a quadratic function relation. In general, the corrosion rate of three steel in the desulfurizing MEDA solution increased with the increase in temperature.

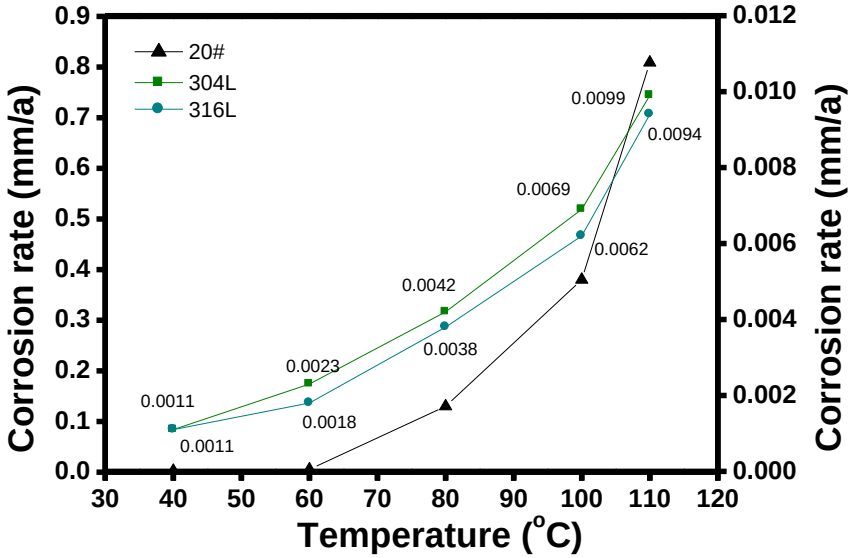


**Figure 3.** Comparative Analysis results of corrosion rate on three different steels at different temperatures

Temperature, as one of operation parameters, brings great challenges to carbon steel (20#), between 110°C to 120°C, at which the desorption of acid gases ($H_2S/CO_2$) occurred in amine liquid regenerator section, bottom reboiler, and the heat exchanger of amine liquid. Thus, taking the material selection design of pipes into consideration, the carbon steel is recommended to be used in the low temperatures zone of desulfurizing equipment. On the contrary, Coating materials for metallurgy pipe of 304L and 316L with excellent corrosion resistance are suitable in the high temperature zone of desulfurizing device [37].

### *3.3 Microanalysis of corrosion*

Figure 4 (left side) shows the SEM surface morphology of corrosion scales on 20# steel. It can be found that at least two layers of corrosion product occurred on the surface of 20# steel in the natural gas sweetening process. The outer layer of the corrosion scale was not dense and the distribution was also nonuniform. However, in contrast to it, the polished lines of raw 304L and 316L steels (nearly 300 magnification times), which can be clearly seen in Figure 5 and 6, indicate mild corrosion.

EDX was used to evaluate the composition of the steel surface. The results (right side) demonstrate the element of the corrosion scale of the surface of three steels. It can be seen that the element of 20# steel such as Fe, S and C appeared in the spectrum of the corrosion scale surface. And rare elements such as Cr and Ni occurred in the corrosion product of 304L and 316L steels which may be responsible for its low corrosion rate.

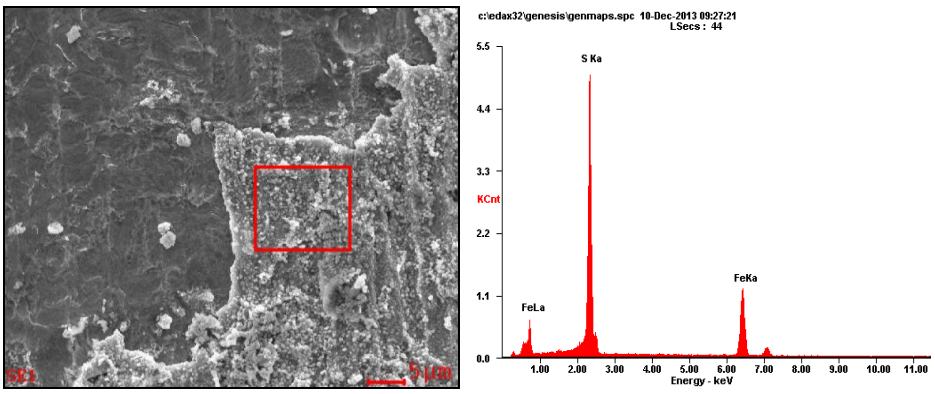


**Figure 4.** SEM-EDS micrographs of 110SS-2Cr steel at 110°C

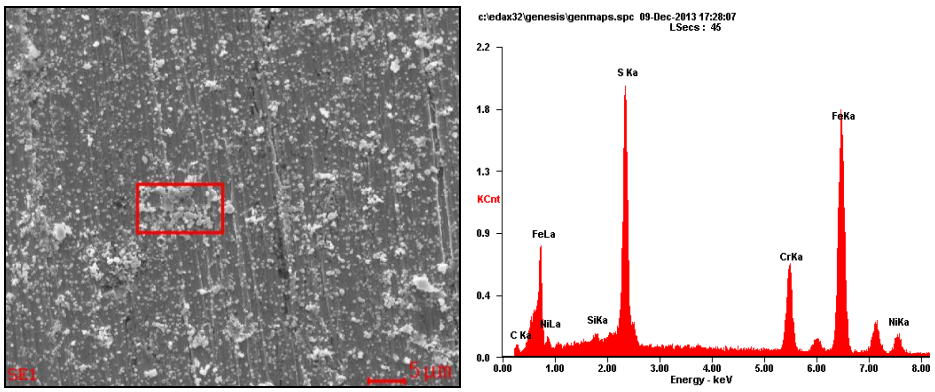


**Figure 5.** SEM-EDS micrographs of 304L steel at 110°C

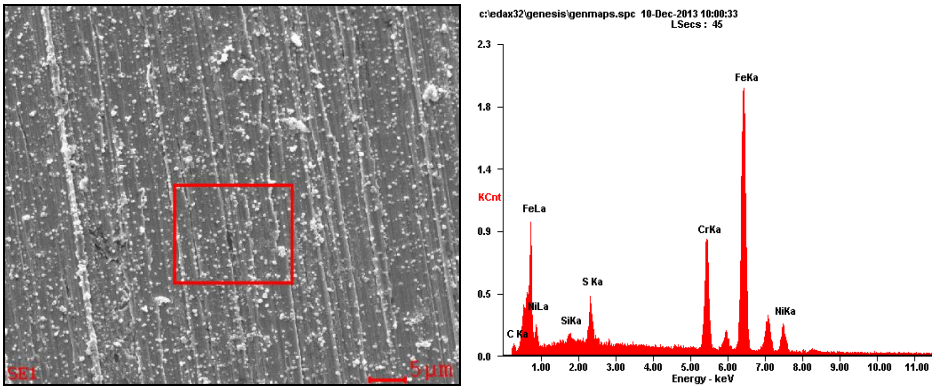


**Figure 6.** SEM-EDS micrographs of 316L steel at 110°C

Due to less corrosion scale, 304L and 316L steel were not used to a detailed XRD analysis. Instead XRD depth profiles of 20# steel were acquired to further clarify the adsorption state of its corrosion scale, as is shown in figure 7. It can be seen that the characteristic diffraction peaks of FeS appeared at the $2\theta$ of 18°, 30°, 39°and 51°. In addition, the bands at 32° and 77° were assigned to the diffraction peak of $FeCO_3$; still a small amount of it indicates $FeS_2$.

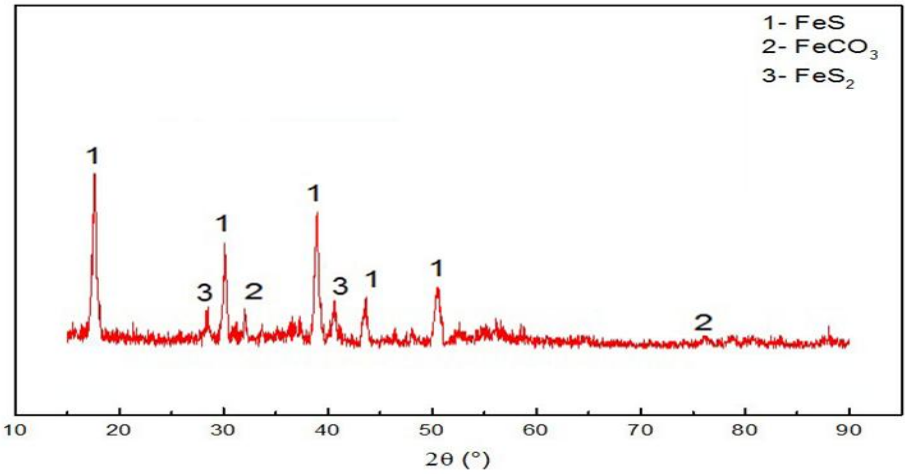


**Figure 7.** XRD spectrum of the corrosion scale on 20 steel

*3.4 Field test*

Field test was carried out to verify indoor experiments in Sichuan natural gas purification plant. The whole operation process of desulfurization device usually appeared as a black box process. Corrosion specimens were fixed in desulfurization equipment, specific installation points are shown in table 4. This experiment was conducted for 981 days, and then the corrosion rate was calculated by the equation 1.

$$v = 87600\frac{\Delta m}{\rho A \Delta t} \quad (1)$$

where, $v$ = corrosion rate (mm/a);
$\Delta m$ = weight loss (g);
$\rho$ = density (g/cm$^3$);
$A$ = surface area (cm$^2$);
$\Delta$t = erosion time (h).

Corrosion rate for inductance probe and coupon was calculated according to the equation 1 and the results are illustrated in table 4. Table 4 also presents the monitoring sites and various operation temperatures during the test for 316L and 20# steels.

Therefore, the two corrosion monitoring methods including inductance probe and coupon test were performed to reveal its corrosion condition. The corrosion monitoring system using inductance probe (model: CR-2000 designed by Chinese Academy of Sciences), featuring short response time and high definition due to the continuous monitoring, has been widely used in corrosion monitoring. The inductance probe and the coupon were combined together in a specific position to measure the corrosion rate through exerting a constant alternating current coil; the coil inductance is very sensitive to changes of the thickness of the metal, which greatly improves the sensitivity of the measurement. The distribution of main monitoring points of the desulfurized equipment in the purification plant is shown in figure 10. It depicts the route of flow with the temperature range of different steel in MDEA solution.

The results show that the two assessment methods are basically the same, except for measurement errors (table 4). In addition, the carbon steel is relatively susceptible to severe corrosion; however, stainless steel is susceptible to slight corrosion. CL-1 to CL-8 is different monitoring sites in the schematic diagram with inlet and outlet pipelines (figure 8). As is observed from table 4 that at CL-1 and CL-2 corrosion rate is 0 mm/a while at CL-3 the corrosion rate is 0.0050 mm/a for coupon and 0.0007 for inductance probe (due to the hydrolysis reactor). Similarly, for CL-4 and Cl-5 no corrosion rate was seen whereas for CL-6 0.0290 mm/a was observed for the 20# steel. Comparing the different disposed area of the 316L material (CL-1 and CL-3), we draw a conclusion that the corrosion rate increases with the increase in temperature [38-40].

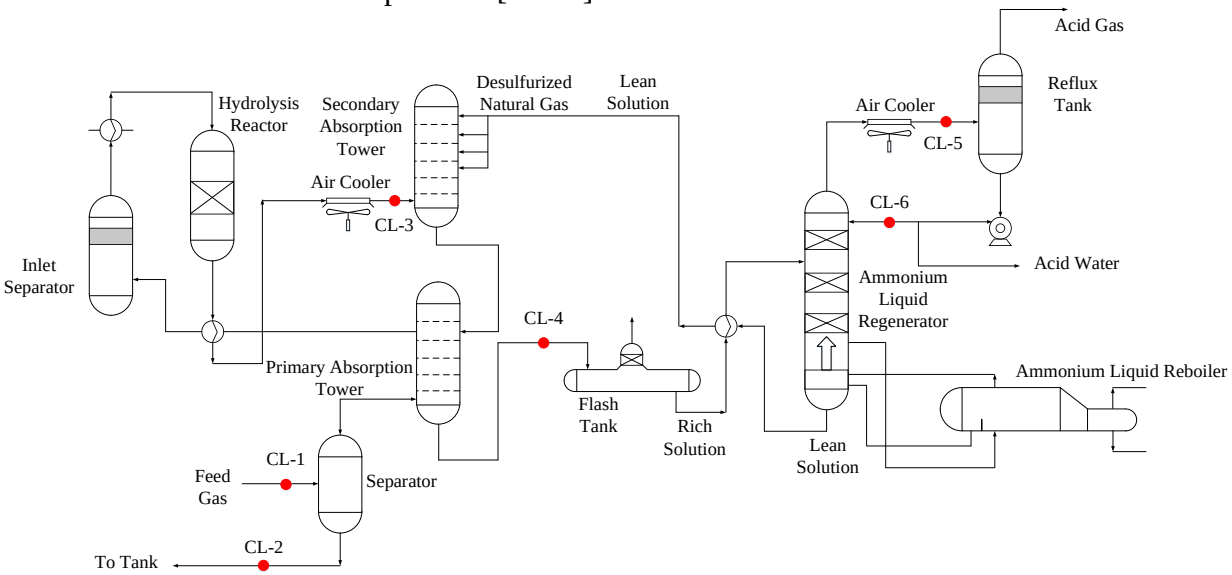


**Figure 8.** Schematic diagram of the distribution of main monitoring points of the desulfurized equipment in the purification plant

**Table 4.** The statistical results of corrosion rate

| Number | Monitoring sites | Operating temperature (°C) | Material | Corrosion rate (mm/a) | |
|---|---|---|---|---|---|
| | | | | Coupon | Inductance probe |
| CL-1 | inlet pipeline | 30-40 | 316L | 0 | 0 |
| CL-2 | liquid outlet pipeline at the bottom of filter separator | 30-40 | 316L | 0 | 0 |
| CL-3 | outlet pipeline of air cooler at hydrolysis reactor outlet | 50 | 316L | 0.0050 | 0.007 |
| CL-4 | Fluid turbine outlet line | 59 | 316L | 0 | 0 |
| CL-5 | outlet pipeline of air cooler on amine liquid regenerator | 50 | 316L | 0 | 0 |
| CL-6 | reflux pipeline on amine liquid regenerator | 50 | 20# | 0.0290 | 0 |

## 4. CONCLUSION

(1) The electrochemical tests showed that: In the MDEA desulfuration solution containing $H_2S$ / $CO_2$, 20 #, 304L and 316L steels are mainly susceptible to $H_2S$ corrosion. With the increase in temperature, the corrosion potentials of the three steels shift negatively, the charge transfer resistance decreases, which accelerate the metal anode dissolution rate significantly. Among them, the 20 # steel corrosion current density varies more with temperature. Compared with 304L, 316L steel contains a certain amount of Mo element which can help forming a passivation film of better stability, has a better resistance ability of pitting corrosion and better performance in the desulfurization solution containing $Cl^-$.

(2) Indoor autoclave loss tests showed that at a lower temperature (40°C ~ 60°C), corrosion rate of 20 #, 304L and 316L are low, but increased significantly as the temperature rises.

(3) Field tests verified that the detection point unit pipelines suffered from relatively severe corrosion are mostly carbon steel, stainless steel corrosion relatively minor. And the corrosion rate increases with increasing temperature. Therefore, carbon material is recommended in the low temperature zone of desulfurization unit to prolong its life by increasing its corrosion allowance, while the stainless steel is recommended in the high temperature zone.

ACKNOWLEDGEMENT
The authors acknowledge the support from national science and technology major projects of China (No. 2011ZX05017), the national natural science foundation of China (No. 51474187), Sichuan 1000 Talent Fund and Open Fund (PLN1411) of State Key Laboratory of Oil and Gas Reservoir Geology and Exploitation, Southwest Petroleum University, Chengdu, China.

## References

1. Z. Feng, Fang Cheng-Gang, Wu You-Ting, Wang Yuan-Tao, Li Ai-Min, Zhang Zhi-Bing, *Chem. Eng. J.* 160 (2010) 691
2. R. W. Baker, *Ind. Eng. Chem. Res*. 41 (2002) 1393
3. Jiazong Jianga, Bo Zhao Yuqun Zhuo, Shujuan Wang, *Int. J. Greenhouse Gas Cont*. 29 (2014) 135
4. Priyabrata Pal, Ahmad AbuKashabeh , Sameer Al-Asheh, Fawzi Banat, *J. Nat. Gas Sci. Eng.* 24 (2015) 124
5. O.Younas, F. Banat, *J. Nat. Gas Sci. Eng.* 18 (2014) 247
6. A. Singh, Y. Lin, E.. E. Ebenso, W. Liu, J. Pan, B. Huang, *J. Ind. Eng. Chem.* (2014) http://doi:. 10.1016/j.jiec.2014.09.034
7. J. Han, J .William Carey, J. Zhang, *J. Appl. Electrochem*. 41 (2011) 741
8. Y. Lin, A.Singh, Y. Wu, C. Zhu, H. Zhu, E. E. Ebenso, *J. Tai. Inst. Chem. Eng*. (2014) http:// Doi:. 10.1016/j.jtice.2014.09.023
9. A. Singh, Y. Lin, W. Liu, D. Kuanhai, J. Pan, B. Huang, C. Ren, D. Zeng, *J. Tai. Inst.Chem. Eng*. 45 (2014) 1918
10. K.R. Ansari, M.A. Quraishi, A. Singh, *J. Ind. Eng. Chem*. (2014) http://dx.doi.org/10.1016/j.jiec.2014.10.017
11. I. Ahamad, R. Prasad, M. A. Quraishi, *Corros. Sci.* 52 (2010) 1472

12. K. R. Ansari, Sudheer, A. Singh, M. A. Quraishi, *J. Disp. Sci. Tech.* (2014) http://doi:. 10.1080/01932691.2014.938349
13. A. Singh, I. Ahamad, V. K. Singh, M. A. Quraishi, *J. Solid State Electrochem.* 15 (2011) 1087
14. M. A. Quraishi, A. Singh, V. K. Singh, D. K. Yadav, A. K. Singh, *Mater. Chem. Phys.* 122 (2010) 114
15. K. R. Ansari, M. A. Quraishi, Ambrish Singh, *Corros Sci.* 79 (2014) 5
16. X.P. Guo, Y. Tomoe, *Corros. Sci.* 41 (1999) 1391
17. G.A. Zhang, Y.F. Cheng, Corros. Sci. 51 (2009) 87
18. Amir Samimi, Mahbobeh Afkhami, *Int. J. Bas.Appl. Sci.* 1 (2013) 594
19. R. Eustaquio-Rincón, M. E. Rebolledo-Libreros, A. Trejo, R. Molnar, *Ind. Eng. Chem. Res*. 47 (2008) 4726
20. F.Y. Jou, A. E. Mather, F. D. Otto, *Ind. Eng. Chem. Process Des. Dev.* 21 (1982) 539
21. X. Hong-Jian, Z. Cheng-Fang , Z. Zhi-Sheng, *Ind. Eng. Chem. Res*. 41 (2002) 2953
22. Y. A. Anufrikov, G. L. Kuranov, N. A. Smirnova, *Rus. J.Appl. Chem*. 80 (2007) 515
23. N. Verma, A. Verma, *Fuel Proces. Tech*. 90 (2009) 483
24. A. Kazemi, M. Malayeri, A. G. Kharaji, A. Shariati, *J. Nat. Gas Sci. Eng*. 20 (2014) 16
25. A. Haghtalab, A. Izadi, *Fluid Phas. Equil*., 375 (2014) 181
26. N. G. Kandile, T. M.A. Razek, A. M. Al-Sabagh, M.M.T. Khattab, *Egypt. J.Petro*. 23 (2014) 323
27. S. Mazinani, A. Samsami, A. Jahanmiri, A.R. Sardarian, *Fluid Phas. Equil*. 305 (2011) 39
28. M. M. Ghiasi, A. H. Mohammadi, *J. Nat. Gas Sci. Eng*. 18 (2014) 39
29. N. Zhang, Dezhi Zeng, Guoqing Xiao, Jianfeng Shang , Yuanzhi Liu, Decai Long, Qiyao He, Ambrish Singh, *J. Nat. Gas Sci. Eng.* 30 (2016) 444
30. Tohid Nejad Ghaffar Borhani, Morteza Afkhamipour, Abbas Azarpour, Vahid Akbari, Seyed Hossein Emadi, Zainuddin A. Manan, *J. Ind. Eng. Chem.* 34 (2016) 344
31. R. Yusoff, A. Shamiri, M.K. Aroua, A. Ahmady, M.S. Shafeeyan, W.S. Lee, S.L. Lim, S.N.M. Burhanuddin, *J. Ind. Eng. Chem.* 20 (2014) 3349
32. A. Erfani, S. Boroojerdi, A. Dehghani, M. Yarandi, *Petr. Coal.* 57 (2015) 48
33. M. A. Karimi, M. Hasheminasab, *Int. J. Electrochem. Sci.* 8 (2013) 4560
34. B. S. Ali, B. H. Ali, R. Yusoff, M. K. Aroua, *Int. J. Electrochem. Sci.* 7 (2012) 3835
35. B. Hamah-Ali, B. S. Ali, R. Yusoff, M. K. Aroua, *Int. J. Electrochem. Sci*. 6 (2011) 181
36. Dong Fu, Pan Zhang, ChenLu Mi, *Energy* 101 (2016) 288
37. Stefania Moioli, Antonio Giuffrida , Matteo C. Romano, Laura A. Pellegrini, Giovanni Lozza, *Appl.Energ.* 183 (2016) 1452
38. S. Jianfeng, L. Tan, L.Yuanzhi, L. Hongqing, Z. Xiaogang, X. Guoqing, *Natur. Gas Ind*. 34 (2014) 134
39. C. Changjie, H. Jinlong, W. Chongrong, *Natur. Gas Ind*. 33 (2013) 112
40. X. Ning, J. Fang, S. Daiyan, *Natur. Gas Ind*. 30 (2012) 70